Environment-Aware Codebook Design for RIS-Assisted MU-MISO Communications: Implementation and Performance Analysis

Zhiheng Yu, Jiancheng An, *Member, IEEE,*

Ertugrul Basar, *Fellow, IEEE*, Lu Gan, and Chau Yuen, *Fellow, IEEE*

Abstract

Reconfigurable intelligent surface (RIS) provides a new electromagnetic response control solution, which can proactively reshape the characteristics of wireless channel environments. In RIS-assisted communication systems, the acquisition of channel state information (CSI) and the optimization of reflecting coefficients constitute major design challenges. To address these issues, codebook-based solutions have been developed recently, which, however, are mostly environment-agnostic. In this paper, a novel environment-aware codebook protocol is proposed, which can significantly reduce both pilot overhead and computational complexity, while maintaining expected communication performance. Specifically, first of all, a channel training framework is introduced to divide the training phase into several blocks. In each block, we directly estimate the composite end-to-end channel and focus only on the transmit beamforming. Second, we propose an environment-aware codebook generation scheme, which first generates a group of channels based on statistical CSI, and then obtains their corresponding RIS configuration by utilizing the alternating optimization (AO) method offline. In each online training

This article was presented in part at the IEEE VTC2024-Spring [1]. This work was partially supported by Sichuan Science and Technology Program under Grant 2023YFSY0008 and 2023YFG0291. The work of Ertugrul Basar was supported by TUBITAK under Grant 120E401. The work of Chau Yuen was supported in part by the Ministry of Education, Singapore, under its Ministry of Education (MOE) Tier 2 under Award MOE-T2EP50220-0019; and in part by the Science and Engineering Research Council of Agency for Science, Technology and Research (A*STAR) Singapore, under Grant M22L1b0110.

Z. Yu and L. Gan are with the national key laboratory on blind signal processing. School of Information and Communication Engineering, University of Electronic Science and Technology of China (UESTC), Chengdu 611731, China, and also with the Yibin Institute of UESTC, Yibin 644000, China (e-mail: zhihengyu2000@163.com; ganlu@uestc.edu.cn).

J. An and C. Yuen are with the School of Electrical and Electronics Engineering, Nanyang Technological University, Singapore 639798 (e-mail: jiancheng_an@163.com; chau.yuen@ntu.edu.sg).

E. Basar is with the Communications Research and Innovation Laboratory (CoreLab), Department of Electrical and Electronics Engineering, Koç University, Sariyer, Istanbul 34450, Turkey. (e-mail: ebasar@ku.edu.tr).

block, the RIS is configured based on the corresponding codeword in the environment-aware codebook, and the optimal codeword resulting in the highest sum rate is adopted for assisting in the downlink data transmission. Third, we analyze the theoretical performance of the environment-aware codebook-based protocol taking into account the channel estimation errors. Finally, numerical simulations are provided to verify our theoretical analysis and the performance of the proposed scheme. In particular, the simulation results demonstrate that our protocol is more competitive than conventional environment-agnostic codebooks.

Index Terms

Reconfigurable intelligent surface (RIS), channel training, environment-aware codebook, multiuser downlink beamforming.

I. Introduction

Reconfigurable intelligent surface (RIS) is an artificial electromagnetic (EM) material with programmable EM properties [2]. Essentially, an RIS is composed of numerous sophisticatedly designed EM meta-atoms. By dynamically adjusting the control signals for each RIS element, it becomes possible to intelligently manipulate the EM characteristics, including the amplitude, phase, polarization, and frequency of the incident signal in a programming manner [3], [4]. In contrast to conventional wireless technologies such as massive multiple-input multiple-output (MIMO) and millimeter wave (mmWave) communications [5] that have to grapple with issues related to network energy consumption and hardware costs, the RIS elements are passive and simply reflect incident signals, mitigating the power-thirsty radio frequency (RF) chains and forward delay in traditional relays [6]–[8]. Remarkably, an RIS can operate in full-duplex mode without encountering self-interference problems [9]. By adjusting the phase shifts at the RIS, various functionalities such as secure communications, focused beam emission, and enhanced indoor coverage can be achieved [10]–[12]. In addition to the single-layer RIS, the application of stacked intelligent metasurfaces (SIM) in different scenarios has also begun to emerge for performing signal processing tasks in the wave domain [13]–[15]. Besides, integrating RIS with transceivers also attracts increased attention [16]. Given these advantages, RIS-empowered

communication is considered to be a key technology enabling future wireless networks [2], [17]–[20].

Nevertheless, RIS-assisted wireless communication systems also present some challenges. On the one hand, obtaining accurate channel state information (CSI) is much more difficult due to the fact that most RISs are composed of passive elements or only equipped with a small number of onboard signal processing units [21], [22]. More specifically, it becomes impractical to separately estimate base station (BS)-RIS and RIS-user channels using traditional pilot-based methods. Therefore, several advanced channel estimation techniques have been proposed to estimate cascaded or composite end-to-end channels [23]–[30]. For instance, *Mishra et al.* introduced a simple ON/OFF method capable of estimating the cascaded BS-RIS-user channels one by one [25]. Subsequently, *Xu et al.* proposed a novel ON/OFF based minimum mean square error (MMSE) channel estimation method for RIS-assisted high mobility systems, which mitigates the Doppler-induced error floor [26]. In order to reduce the pilot overhead required for estimating the cascaded BS-RIS-user channels, *Wang et al.* leveraged the similarity of the BS-RIS link between multiple users [24]. Furthermore, in [27], *Wei et al.* considered the double-structured sparsity of the cascaded channels to estimate the angle parameters, while [23] proposed a channel training-based scheme to directly estimate the composite channels. More recently, *Guo et al.* developed a new channel estimator leveraging the unitary approximate message passing (UAMP) technique [28], and *Chen et al.* proposed a new compressed sensing-based channel estimation protocol to estimate the cascaded channels [29], [31]. Combined with deep learning, *Xu et al.* proposed a three-stage joint channel decomposition and prediction framework that exploits the quasi-static property of BS-RIS channel and the fast time-varying property of RIS-user channels [30].

On the other hand, the optimization of reflecting coefficients (RCs) at the RIS constitutes another challenge [32]–[40]. More specifically, in [34], *Wu and Zhang* concentrated on minimizing the total transmit power under specific signal-to-interference-plus-noise ratio (SINR) constraints, they adopted alternating optimization (AO) method based on semidefinite relaxation (SDR) to obtain approximate solutions of transmit precoding matrix and RIS RCs. In [32], *Yan et al.* devised RCs based on the statistical CSI to maximize spectral efficiency. In [37], *Di et al.* proposed a hybrid beamforming scheme to maximize the sum rate of RIS-aided multi-

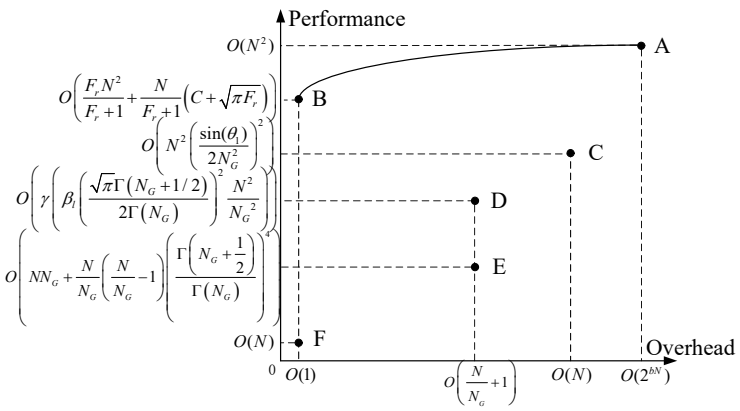
TABLE I
COMPARISON OF PROPOSED SCHEME WITH RECENT RIS SOLUTIONS

Reference	MIMO setup	Phase shift model	Optimization objective	Channel	Complexity	Imperfect CSI	PBF design
Proposed	MU-MISO	Discrete	Sum rate	Composite	Low	✓	✓
[23]	MU-MIMO	Discrete	Transmit power	Composite	Low	✓	✓
[33]	MIMO	Discrete	Throughput	Composite	Low	✓	✓
[34]	MU-MISO	Continuous	Transmit power	Separate	High	×	×
[17]	MIMO	Continuous	Throughput	Separate	High	×	✓
[41]	MIMO	Discrete	Received signal power	Separate	Moderate	×	✓
[42]	MISO	Discrete	Achievable rate	Composite	Low	✓	✓
[27]	MU-MISO	Continuous	NMSE	Separate	Moderate	×	×
[38]	MIMO	Discrete	ASE	Separate	Moderate	✓	✓
[28]	MIMO	Continuous	NMSE	Separate	Low	×	×
[24]	MU-MISO	Continuous	NMSE	Separate	Moderate	✓	×

ASE: Average spectral efficiency NMSE: Normalized mean square error PBF: Passive beamforming

user multiple-input single-output (MU-MISO) systems. For beyond-diagonal (BD) RIS-aided multi-user systems, *Fang and Mao* proposed a closed-form solution for passive beamforming to maximize the sum of the effective channel gains [40]. Besides, [36] proposed a heuristic algorithm to optimize continuous phase shifts of RIS-aided massive MIMO systems. In an RIS-aided mmWave MIMO system, *Xu et al.* developed a novel deep reinforcement learning (DRL) algorithm to design joint beamforming according to a location-aware imitation environment [39]. However, it is important to note that the schemes mentioned above assume the perfect CSI, which is generally unavailable in practical scenarios. Considering the imperfect CSI, in [33], *An et al.* conceived a low-complexity framework for maximizing the achievable rate of RIS-aided MIMO system with discrete phase shifts. The RCs are pre-designed and the effective composite channel is estimated. Moreover, [35] considered an imperfect CSI scenario and solved the max-min SINR problem considering a continuous phase shift. In [38], *Nikolaos et al.* proposed two phase shift design schemes whose complexity is linear to the number of RIS elements and receive antennas.

In addition, considering the complexity and overhead, [45] proposed a low-complexity antenna selection algorithm to avoid the joint optimization problem with the transceiver, which is capable of supporting arbitrary MIMO configuration. Moreover, several group-/fully-connected schemes are introduced to reduce the pilot overhead. More specifically, in [43], *Shen et al.* proposed a novel RIS architecture based on group- and fully-connected reconfigurable impedance networks



A [34]: Optimal configuration B [42]: Statistic CSI-based scheme
C [41]: Scalar/Vector RIS design D [43]: Optimal RIS grouping
E [44]: Group connected RIS F [34]: Random configuration
B-A curve: Proposed environment-aware codebook scheme
F_r : Rician factor of the RIS-user channel
C : Euler-Mascheroni constant
θ_1 : RC angle of the reactance matrix's non-zero eigenvalues
γ : Transmit SNR
Γ : Gamma function
N_G: Number of RIS elements in each group
β_l : Large-scale path loss coefficient of the cascaded link

Fig. 1. The performance versus overhead diagram, where the proposed scheme strikes a flexible tradeoff between the statistical CSI-based scheme and the optimal RIS configuration.

and derived the scaling law for received signals in RIS-aided MIMO systems. Adopting a similar RIS structure, [41] analyzed the scaling law for received signal power using BD RISs in case of discrete phase shifts. Additionally, in [44], *Kundu et al.* adopted a grouping strategy to optimize the RIS and derived a tight closed-form upper bound for the achievable rate.

Recently, various codebook-based schemes have emerged to enhance RIS-based systems' performance with moderate overhead. For instance, [46] proposed a codebook-based framework and introduced three codebook generation schemes. Further in [22] and [23], *An et al.* employed a low complexity framework to maximize the achievable rate. They analyzed the theoretical performance of the random and uniform codebooks. Beyond generating codebooks offline, in [42], *Jia et al.* proposed an environment-aware codebook design to flexibly adapt to different channel conditions. Moreover, [47] proposed a discrete Fourier transform (DFT) codebook, which, however, experiences significant SINR loss in the near-field region of RIS [48]. To solve this problem, a ring-type codebook based on the Fresnel principle was further proposed to determine the phase distribution by employing the location information of the user and an RIS.

Besides, in [49], *Abdallah et al.* developed a multi-agent DRL-based beamforming codebook design that relies only on receiving power measurements.

Nevertheless, the above codebook-based schemes usually entail substantial training overhead and lack adaptability to channel environment variations. Against this background, in this paper, we introduce a novel codebook-based protocol for RIS-assisted MU-MISO systems and propose an environment-aware scheme to obtain a discrete RIS RC configuration codebook. Specifically, we first generate virtual channels in each training block according to the statistical CSI, and then perform AO of RC configuration and transmit power allocation to obtain the corresponding RIS RC codeword. In the on-line stage, we configure the RIS according to the predesigned codebook and estimate the composite end-to-end channel for each codeword, which reduces the performance loss caused by imperfect CSI. Then, we theoretically analyze the received power scaling law in a single-user scenario considering both the perfect and imperfect CSI to gain valuable insights into the proposed environment-aware codebook scheme. Comparing with the existing work [42], we derive a tighter upper bound of the achievable rate in perfect CSI scenario. Moreover, the influence of channel estimation errors in the environment-aware codebook-based schemes has been theoretically analyzed in *Proposition 2*. For illustration, we contrast the proposed scheme to its existing channel estimation and passive beamforming counterparts in Table I. In addition, as shown in Fig. 1, we show the performance vs. overhead tradeoff of the proposed scheme and contrast it to existing schemes. To summarize, our contributions are outlined as follows.

1) We propose a channel training-based protocol for RIS-assisted MU-MISO systems. In contrast to conventional schemes, we develop a novel environment-aware codebook design scheme, where we generate a set of virtual channels with the same distribution as practical channels. For each virtual channel, we employ the AO method to solve the sum rate maximization problem. Specifically, we adopt a successive refinement method to optimize the RC at the RIS and a classic water-filling power allocation algorithm to allocate transmit power at the BS when one of them is fixed. By doing so for Q virtual channels, we generate an environment-aware RC codebook.
2) Then, in the on-line stage, we configure the RIS using each codeword in the environment-

aware codebook and thus obtain Q candidate composite end-to-end channels. The optimal index that maximizes the sum rate is determined to obtain the corresponding discrete RIS configuration and transmit power allocation.

3) Next, the theoretical achievable rate adopting the proposed environment-aware channel training-based protocol is analyzed under both the perfect and imperfect CSI scenarios. To the best of our knowledge, this is the first work to analyze the influence of channel estimation errors on codeword index selection.
4) Finally, numerical simulation results are provided to validate our performance analysis. Both the theoretical analysis and simulation results demonstrate that the proposed environment-aware codebook scheme strikes a flexible trade-off between the achievable performance and pilot overhead.

The rest of this paper is organized as follows. Section II introduces the RIS-assisted multi-user system model. In Section III, we introduce the proposed codebook-based protocol and environment-aware codebook generation scheme. Then, the theoretical performance of the proposed scheme is analyzed in Section IV, where the effects of channel estimation errors are also considered. Section V provides numerical simulations to evaluate the performance of the proposed scheme. Finally, Section VI concludes the paper.

Notations: Scalars are denoted by italic letters, vectors and matrices are denoted by lower and upper bold-face letters, respectively; $\mathbb{C}^{x\times y}$ denotes the space of $x \times y$ complex-valued matrices; For any general matrix $\mathbf{A}$, $\mathbf{A}^T, \mathbf{A}^H, \mathbf{A}^*, \text{rank}(\mathbf{A})$ represent its transpose, Hermitian transpose, conjugate and rank, respectively; For a complex-valued vector $\mathbf{x}$, $\|\mathbf{x}\|$ denotes its Euclidean norm, $|\mathbf{x}|$ denotes its magnitude, and $\text{diag}(\mathbf{x})$ denotes a diagonal matrix with each diagonal element being the corresponding entry in $\mathbf{x}$; We denote the $N \times N$ identity matrix as $\mathbf{I}_N$; $\log(\cdot)$ and $\lfloor\cdot\rfloor$ represent the logarithmic function and floor operator, respectively; The distribution of a circularly symmetric complex Gaussian (CSCG) random vector with mean vector $\mathbf{x}$ and covariance matrix $\mathbf{\Sigma}$ is denoted by $\sim \mathcal{CN}(\mathbf{x}, \mathbf{\Sigma})$, where $\sim$ stands for "distributed as"; For a square matrix $\mathbf{S}$, $\text{tr}(\mathbf{S})$ and $\mathbf{S}^{-1}$ denote its trace and inverse, respectively; $\mathbb{E}\{\cdot\}$ denotes the statistical expectation. $\Re\{\cdot\}$ and $\Im\{\cdot\}$ denotes the real part and imagine part of a complex number, respectively. For clarity, we summarize the main symbols used in this paper and their meanings in Table II.

TABLE II
MAJOR SYMBOLS AND THEIR MEANINGS

Symbol	Meaning
M	The number of BS antennas
N	The number of RIS elements
K	The number of users
Q	Training overhead
$\mathbf{G}$	The BS-RIS channel
$\mathbf{h}_{d,k}^H$	The BS-user k channel
$\mathbf{h}_{r,k}^H$	The RIS-user k channel
$\mathbf{h}_k^H$	The composite channel of user k
$\mathbf{\Phi}$	RC configuration of the RIS
$\mathbf{w}$	Transmit precoding vector
θ	Phase shift of RIS element
R	Sum rate of multiple users
T_c	The channel coherence time
$\overline{\mathbf{P}}$	Transmit power allocation matrix
ε	Composite channel estimation error
P_d	Transmit power at the BS
P_{ul}	Average power of the pilot signals
σ_z^2	Average noise power at the BS
σ_k^2	Average noise power at the users

II. SYSTEM MODEL

Let us consider an RIS-assisted multi-user communication system in a single cell as shown in Fig. 2, where an RIS with N reflecting elements is deployed to enhance the downlink (DL) signal transmission between a multi-antenna BS and K single-antenna users. The number of transmit antennas at the BS is denoted by M. The RIS is equipped with a smart controller capable of adjusting the RCs according to the real-time CSI [21]. In this paper, we adopt a quasi-static flat-fading channel model for all links. Besides, we consider a time-division duplexing (TDD) protocol for both uplink (UL) as well as DL transmissions and assume the channel's reciprocity for the CSI acquisition in the DL based on the UL training. The baseband equivalent channels

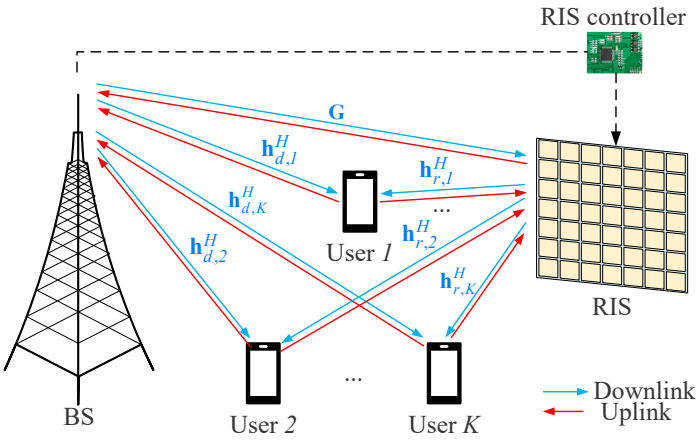


Fig. 2. An RIS-assisted multiuser communication system.

spanning from the BS to the RIS, from the RIS to user k, and from the BS to user k are denoted by $\mathbf{G} \in \mathbb{C}^{N\times M}$, $\mathbf{h}_{r,k}^H \in \mathbb{C}^{1\times N}$, $\mathbf{h}_{d,k}^H \in \mathbb{C}^{1\times M}$, respectively, with $k = 1, 2, \cdots, K$.

Let the diagonal matrix $\mathbf{\Phi} = \text{diag}\left(\varphi_1, \varphi_2, \cdots, \varphi_N\right)$ represent the RC configuration of the RIS, where φ_n denotes the RC of the nth RIS element, following $|\varphi_n| = 1$ for $n = 1, 2, \cdots, N$. In this paper, we use discrete phase shifts to control signal reflection. In order to facilitate the practical implementation, we consider that the discrete phase shifts are obtained by uniformly quantizing the interval $[0, 2\pi)$ and let b represent the number of bits used for quantizing the phase shift levels. Hence the phase shift of each RIS element is assumed to be one of $B = 2^b$ discrete phase shift values. The phase shift set $\mathcal{B}$ is given by

$$\mathcal{B} = \{0, \Delta\theta, \cdots, (B-1)\Delta\theta\}, \tag{1}$$

where $\Delta\theta = 2\pi/B$. Thus, the RC of the nth element at the RIS can be expressed as $\varphi_n = e^{j\theta_n}$, $\theta_n \in \mathcal{B}$, $n = 1, 2, \cdots, N$ and the composite end-to-end channel for user k is given by

$$\mathbf{h}_k^H = \mathbf{h}_{r,k}^H \mathbf{\Phi} \mathbf{G} + \mathbf{h}_{d,k}^H, \quad k = 1, 2, \cdots, K. \tag{2}$$

Let $\mathbf{H} = [\mathbf{h}_1, \mathbf{h}_2, \cdots, \mathbf{h}_K] \in \mathbb{C}^{M\times K}$ represent the UL channels associated with K users.

During the channel estimation process in the UL phase, the pilot signal received at the BS is

given by

$$\mathbf{y} = \sum_{k=1}^{K} \mathbf{h}_k \sqrt{P_{\text{ul}}} x_k + \mathbf{z}, \tag{3}$$

where P_{ul} is the average power of the pilot symbols, which is assumed to be identical for all users, x_k denotes the pilot symbol transmitted from user k to BS with zero mean and unit variance, $\mathbf{z} \in \mathbb{C}^{M\times 1}$ denotes the additive white Gaussian noise (AWGN) at the BS obeying $\mathbf{z} \sim \mathcal{CN}(\mathbf{0}, \sigma_z^2 \mathbf{I}_M)$.

Next, we consider the DL of data transmission and use linear transmit precoding at the BS. As a result, the complex baseband signal received at user k is given by

$$r_k = \mathbf{h}_k^H \sum_{i=1}^{K} \mathbf{w}_i s_i + n_k, \tag{4}$$

where s_k denotes the transmitted information symbol of user k, $\mathbf{w}_k \in \mathbb{C}^{M\times 1}$ denotes the corresponding transmit beamforming vector and $n_k \sim \mathcal{CN}(0, \sigma_k^2), k = 1, 2, \cdots, K$ denotes the AWGN at the kth user's receiver.

Meanwhile, we adopt the Rician channel in this paper. Specifically, the RIS-user k channel can be expressed as

$$\mathbf{h}_{r,k} = \sqrt{\beta_r} \left(\sqrt{\frac{F_r}{F_r+1}} \mathbf{h}_{r,k}^{\text{LoS}} + \sqrt{\frac{1}{F_r+1}} \mathbf{h}_{r,k}^{\text{NLoS}} \right), \tag{5}$$

where β_r and F_r are the path loss and the Rician factor of RIS-user channel, respectively; $\mathbf{h}_{r,k}^{\text{LoS}}$ and $\mathbf{h}_{r,k}^{\text{NLoS}}$ represent the line-of-sight (LoS) and non-line-of-sight (NLoS) components of RIS-user channel, respectively. The NLoS components are i.i.d. complex Gaussian variables with zero mean and unit variance, satisfying $\mathbf{h}_{r,k}^{\text{NLoS}} \sim \mathcal{CN}(\mathbf{0}, \mathbf{I}_N)$. Similarly, the BS-user channel and BS-RIS channel are modeled by using (5).

Moreover, we consider a uniform linear array (ULA) of M antennas at the BS and a uniform planar array (UPA) of N antennas at the RIS. Let $\mathbf{a}_{\text{BS}}(\delta) \in \mathbb{C}^{M\times 1}$ and $\mathbf{a}_{\text{R}}(\zeta, \gamma) \in \mathbb{C}^{N\times 1}$ denote the steering vector of the BS and the RIS, respectively. Specifically, the mth entry of $\mathbf{a}_{\text{BS}}$ is denoted as $e^{j\frac{2\pi}{\lambda}(m-1)d_{\text{BS}}\sin(\delta)}, m = 1, 2, \cdots, M$, where d_{BS} denotes the element spacing of the BS, λ denotes the wavelength of the signal, and $\delta \in [-\pi/2, \pi/2)$ de-

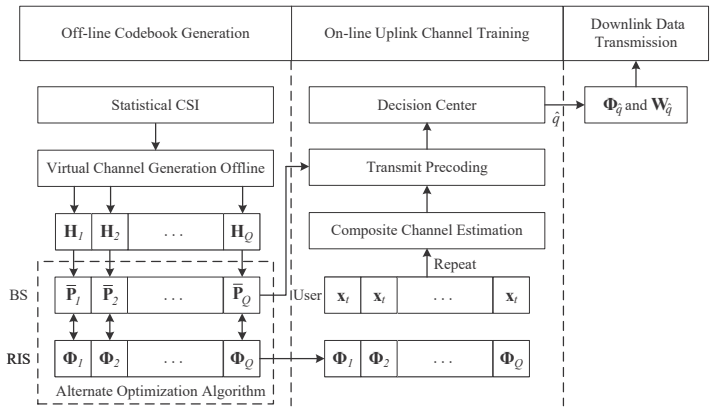


Fig. 3. The frame structure of the proposed protocol.

notes the angle of departure (AoD) or the angle of arrival (AoA). The nth entry of $\mathbf{a}_{\mathrm{R}}$ is denoted as $e^{j\frac{2\pi}{\lambda}d_{\mathrm{R}}\sin(\gamma)\left[\lfloor\frac{n-1}{N_x}\rfloor\sin(\zeta)+((n-1)-\lfloor\frac{n-1}{N_x}\rfloor N_x)\cos(\zeta)\right]/\lambda}, n=1,2,\cdots,N$, where d_{R} denotes the element spacing of the RIS. N_x is the number of reflecting elements deployed at each row of the RIS. Moreover, $\zeta \in [0,\pi)$ and $\gamma \in [-\pi/2,\pi/2)$ denote the azimuth and elevation AoA/AoD, respectively. Thus, the LoS component of the $\mathbf{G}$, $\mathbf{h}_r$ and $\mathbf{h}_d$ are given by $\mathbf{a}_{\mathrm{BS}}\left(\delta_d^{\mathrm{AoA}}\right)$, $\mathbf{a}_{\mathrm{R}}\left(\zeta_g^{\mathrm{AoA}},\gamma_g^{\mathrm{AoA}}\right)\mathbf{a}_{\mathrm{BS}}\left(\delta_g^{\mathrm{AoD}}\right)^H$ and $\mathbf{a}_{\mathrm{R}}\left(\zeta_r^{\mathrm{AoA}},\gamma_r^{\mathrm{AoA}}\right)$, respectively, where δ_d^{AoA} and δ_g^{AoD} represent the AoA from the user to the BS and the AoD from the BS to the RIS, respectively; ζ_g^{AoA} and γ_g^{AoA} represent the azimuth and elevation AoA from the BS to the RIS, respectively; ζ_r^{AoA} and γ_r^{AoA} represent the azimuth and elevation AoA from the user to the RIS, respectively.

III. The Proposed Channel Training Protocol

In this section, we outline the proposed codebook-based scheme by first introducing our channel training-based protocol in Section III-A. Then, our bespoke environment-aware codebook generation scheme is proposed in Section III-B. In Section III-C, we introduce the on-line codebook configuration stage.

A. Channel Training-Based Protocol

As shown in Fig. 3, our channel training-based protocol consists of *off-line* and *on-line* stages.

In the off-line stage, we generate a group of virtual channels based on the statistical CSI. Then, we use the AO algorithm to obtain the optimal RC configuration corresponding to each virtual channel. Repeating for Q virtual channels generates the RC codebook.

In the on-line stage, the transmission protocol is divided into two phases:

- *The UL channel training phase*: During the UL channel training phase, we adjust the RIS configuration over training blocks according to the environment-aware codebook. Then, we repeat carrying out the composite channel estimation and the transmit precoding design to obtain Q candidate channels;
- *The DL data transmission phase*: During the DL signal transmission phase, we select the optimal channel maximizing the sum rate from Q candidates, and get the corresponding RIS configuration and transmit power allocation to assist in the DL communications.

B. Off-Line Codebook Design Stage

Next, we elaborate on the detailed steps to generate the environment-aware codebook.

1) Virtual Channel Generation Based on Statistical CSI: Note that the statistical CSI of all channels is easier to obtain by measurement or averaging historical observations, and it has a longer channel coherence time [32], [50]. In this paper, we utilize the statistical CSI, which includes the path loss, the LoS component and the distribution of the NLoS component of the practical channels to design the environment-aware codebook offline. Specifically, we generate Q virtual channels off-line for the RIS-user k link according to (5), yielding

$$\mathbf{h}_{r,k,q} = \sqrt{\beta_r}\left(\sqrt{\frac{F_r}{F_r+1}}\mathbf{h}_{r,k}^{\mathrm{LoS}} + \sqrt{\frac{1}{F_r+1}}\tilde{\mathbf{h}}_{r,k,q}^{\mathrm{NLoS}}\right), \tag{6}$$

where $\mathbf{h}_{r,k}^{\mathrm{LoS}}$ is the LoS component of the virtual channel and it remains unchanged within each channel coherence block, $\tilde{\mathbf{h}}_{r,k,q}^{\mathrm{NLoS}}$ represents the NLoS component of the qth virtual channel which is randomly generated following the same distribution with $\mathbf{h}_{r,k}^{\mathrm{NLoS}}$ during each training block. In addition, the virtual channels for BS-RIS and BS-user k links are generated in the same way.

2) Alternating Optimization Algorithm: For each tentative virtual channel, we endeavor to maximize the sum rate for all users by jointly optimizing the transmit precoding at the BS and

the RC configuration at the RIS, subject to the total transmit power. Specifically, the optimization problem is formulated as

$$\begin{aligned}
&\max_{\mathbf{W}_q,\mathbf{\Phi}_q} \sum_{k=1}^{K} \log_2\left(1+\frac{\left|\mathbf{h}_{k,q}^H\mathbf{w}_{k,q}\right|^2}{\sum_{l\neq k}^{K}\left|\mathbf{h}_{k,q}^H\mathbf{w}_{l,q}\right|^2+\sigma_k^2}\right)\\
&\text{s.t.}\mathbf{\Phi}_q=\text{diag}\left(\varphi_{q,1},\varphi_{q,2},\cdots,\varphi_{q,N}\right),\\
&\varphi_{q,n}=e^{j\theta_{q,n}},\quad \theta_{q,n}\in\mathcal{B},\quad \forall n\in\mathcal{N},\\
&\sum_{k=1}^{K}\|\mathbf{w}_{k,q}\|^2\leq P_d,
\end{aligned}\tag{7}$$

for $q=1,2,\cdots,Q$, where $\mathbf{h}_{k,q}^H=\mathbf{h}_{r,k}^H\mathbf{\Phi}_q\mathbf{G}+\mathbf{h}_{d,k}^H\in\mathbb{C}^{1\times M}$ and $\mathbf{w}_{k,q}$ are the composite channel and the transmit precoding vector for user k during the qth training block, respectively. $\mathbf{W}_q=[\mathbf{w}_{1,q},\mathbf{w}_{2,q},\cdots,\mathbf{w}_{K,q}]\in\mathbb{C}^{M\times K}$ denotes the transmit precoding matrix. P_d is the total transmit power at the BS.

In this paper, we adopt zero-forcing (ZF) beamforming at the BS to eliminate interference between different users, yielding

$$\begin{aligned}
&\mathbf{h}_{k,q}^H\mathbf{w}_{k,q}=\sqrt{p_{k,q}},k=1,2,\cdots,K,\\
&\mathbf{h}_{k,q}^H\mathbf{w}_{l,q}=0,\forall l\neq k,l=1,2,\cdots,K,
\end{aligned}\tag{8}$$

where $p_{k,q}$ denotes the received power of user k in the qth training block.

Let $\mathbf{H}_q^H=[\mathbf{h}_{1,q},\mathbf{h}_{2,q},\cdots,\mathbf{h}_{K,q}]^H\in\mathbb{C}^{K\times M},q=1,2,\cdots,Q$ represent the DL composite channels in the qth training block, the optimal transmit precoding matrix $\mathbf{W}_q$ is given by a pseudo-inverse of $\mathbf{H}_q^H$ with an appropriate power allocation among users. More specifically, the transmit precoding matrix can be expressed as

$$\mathbf{W}_q=\mathbf{H}_q\left(\mathbf{H}_q^H\mathbf{H}_q\right)^{-1}\mathbf{P}_q^{\frac{1}{2}},\tag{9}$$

where $\mathbf{P}_q=\text{diag}\left(p_{1,q},p_{2,q},\cdots,p_{K,q}\right)$ denotes the received power matrix in the qth training block.

As a result, the sum rate R_q can be simplified as

$$R_q = \sum_{k=1}^{K} \log_2 \left(1 + \frac{p_{k,q}}{\sigma_k^2}\right). \tag{10}$$

Next, we utilize the AO algorithm to obtain the optimal transmit power allocation and RC solution, which consists of the following two parts:

a) Transmit Power Allocation: Given a tentative RIS RC configuration matrix $\mathbf{\Phi}_q$, the transmit power allocated to user k is $\overline{p}_{k,q} = \|\mathbf{w}_{k,q}\|^2$. Let $\mathbf{U}_q = \left(\mathbf{H}_q^H \mathbf{H}_q\right)^{-1} \in \mathbb{C}^{K\times K}$, $\overline{\mathbf{P}}_q = \text{diag}\left(\overline{p}_{1,q}, \overline{p}_{2,q}, \cdots, \overline{p}_{K,q}\right)$ denotes the transmit power allocation matrix. By applying the classic water-filling power allocation algorithm [33], the transmit power allocated to the kth user can be expressed as

$$\overline{p}_{k,q} = \max\left\{\frac{1}{\eta_q} - \sigma_k^2 u_{k,q}, 0\right\}, \tag{11}$$

where $u_{k,q}$ is the kth diagonal element of $\mathbf{U}_q$ and η_q is a threshold that satisfies $\sum_{k=1}^{K} \max\left\{\frac{1}{\eta_q} - \sigma_k^2 u_{k,q}, 0\right\} = P_d$. Once the transmit power allocation among users is obtained, the received power of user k can be expressed as $p_{k,q} = \overline{p}_{k,q}/u_{k,q}$.

b) RIS RC Optimization: Given the transmit power allocation matrix $\overline{\mathbf{P}}_q$, problem (7) is reduced to

$$\begin{aligned} \max_{\theta_{q,n}} \ & R_q(\theta) = \sum_{k=1}^{K} \log_2 \left(1 + \frac{\overline{p}_{k,q}}{u_{k,q}\sigma_k^2}\right) \\ \text{s.t.} \ & \theta_{q,n} \in \mathcal{B}, \forall n \in \mathcal{N}. \end{aligned} \tag{12}$$

In this paper, we adopt a successive refinement method to optimize RIS RCs one by one. Specifically, when fixing other $(N-1)$ RCs, we calculate the objective function value $R_q(\theta)$ for all potential values of $\theta_{q,n}$ in $\mathcal{B}$ and choose the phase shift corresponding to the maximum value. After repeating this one-dimensional search process several times, we obtain the optimal RIS configuration $\mathbf{\Phi}_q$ corresponding to the transmit power allocation $\overline{\mathbf{P}}_q$.

Moreover, we use random phase shifts to initialize power allocation. Then we alternately optimize the power allocation and RIS configuration until the objective function R_q reaches

Algorithm 1 Environment-Aware Codebook Design.

Input: Statistical CSI.

Output: $\mathbf{\Phi}_q$ and $\overline{\mathbf{P}}_q$, $q = 1, 2, \cdots, Q$.

for $q \in \{1, 2, \cdots, Q\}$ **do**
  Generate $\mathbf{h}_{r,k,q}$, $\mathbf{h}_{d,k,q}$, $k = 1, 2, \cdots, K$ and $\mathbf{G}_q$ according to (6).
  Set $r = 1$.
  Initialize the random RC matrix $\mathbf{\Phi}_q^r$.
  repeat
    Optimize $\overline{\mathbf{P}}_q^r$ according to (11).
    for $n \in \{1, 2, \cdots, N\}$ **do**
      Optimize $\varphi_{q,n}^r = e^{j\theta_{q,n}^r}$ according to (12).
    end for
    Update $r = r + 1$.
  until The fractional decrease of R_q is below a threshold $\epsilon > 0$.
  $\mathbf{\Phi}_q = \mathbf{\Phi}_q^r$ and $\overline{\mathbf{P}}_q = \overline{\mathbf{P}}_q^r$.
end for
return $\mathbf{\Phi}_q$ and $\overline{\mathbf{P}}_q$.

convergence.

By carrying out the virtual channel generation in (6) and the AO method for all Q training blocks, we obtain Q candidate channels and their corresponding $\overline{\mathbf{P}}_q$ and $\mathbf{\Phi}_q$. Note that our channels are generated offline according to the statistical CSI, the corresponding RIS configuration and power allocation are also performed offline.

C. On-Line RIS Configuration Stage

In the on-line stage, we complete the RIS configuration by selecting the optimal codeword in the environment-aware codebook to assist in the DL transmission. Specifically, we adjust the RIS RC in different training blocks and obtain Q objective function values. The decision center will select the optimal codeword maximizing the sum rate to assist in the DL data transmission. Accordingly, the transmit precoding matrix is also determined.

1) Composite Channel Estimation: Specifically, given the RC configuration of the qth training block $\mathbf{\Phi}_q$, $q = 1, 2, \cdots, Q$ the received signal at the tth time slot (TS) of the qth training block

is given by

$$\begin{aligned}\mathbf{y}_{q,t} &= \sum_{k=1}^{K} \mathbf{h}_{k,q}\sqrt{P_{\text{ul}}}x_{k,t} + \mathbf{z}_{q,t} \\ &= \sqrt{P_{\text{ul}}}\mathbf{H}_q\mathbf{x}_t + \mathbf{z}_{q,t}, \end{aligned} \tag{13}$$

where $\mathbf{h}_{k,q}$ denotes the composite channel spanning from the kth user to the BS in the qth training block, $x_{k,t}$ is the pilot symbol transmitted from user k to the BS in TS t, which remains identical for all Q training blocks, $\mathbf{x}_t = [x_{1,t}, x_{2,t}, \cdots, x_{K,t}]^T$ is the pilot vector of the tth TS.

Upon collecting the signals of T TSs in the qth training block, the signal received at the BS in this block is given by

$$\mathbf{Y}_q = [\mathbf{y}_{q,1}, \mathbf{y}_{q,2}, \cdots, \mathbf{y}_{q,T}] = \sqrt{P_{\text{ul}}}\mathbf{H}_q\mathbf{X} + \mathbf{Z}_q, \tag{14}$$

where $\mathbf{X} = [\mathbf{x}_1, \mathbf{x}_2, \cdots, \mathbf{x}_T] \in \mathbb{C}^{K\times T}$ is the pilot matrix used for estimating the composite channels spanning from the K users to the BS. $\mathbf{Z}_q = [\mathbf{z}_{q,1}, \mathbf{z}_{q,2}, \cdots, \mathbf{z}_{q,T}] \in \mathbb{C}^{M\times T}$ denotes the noise matrix at the BS during the qth training block.

The composite channel estimation during each block is equivalent to the channel estimation for conventional MU-MISO systems. We employ the mutually orthogonal pilot design to mitigate the interference between multiple users. In order to generate K groups of mutually orthogonal pilot sequences for separating the pilot signals transmitted by K users, the length of the pilot sequence T must satisfy $T \geq K$. Furthermore, to minimize the pilot overhead, we consider $T = K$ [51]. The least squares (LS) estimate of the composite channel $\mathbf{H}_q$ of the qth training block can be expressed as

$$\widetilde{\mathbf{H}}_q = \frac{1}{K\sqrt{P_{\text{ul}}}}\mathbf{Y}_q\mathbf{X}^H. \tag{15}$$

2) Transmit Precoding: Based on the estimate of the composite channel in the qth training block, BS performs multi-user transmit precoding by utilizing the ZF precoder:

$$\widetilde{\mathbf{W}}_q = \widetilde{\mathbf{H}}_q\left(\widetilde{\mathbf{H}}_q^H\widetilde{\mathbf{H}}_q\right)^{-1}\widetilde{\mathbf{P}}_q^{\frac{1}{2}}, \tag{16}$$

where $\widetilde{\mathbf{P}}_q = \text{diag}\left(\widetilde{p}_{1,q}, \widetilde{p}_{2,q}, \cdots, \widetilde{p}_{K,q}\right)$ is the received power allocation matrix and $\widetilde{p}_{k,q} = \frac{\overline{p}_{k,q}}{\widetilde{u}_{k,q}}$ is the received power of user k when configuring the qth codeword, $\widetilde{u}_{k,q}$ is the kth diagonal element of $\widetilde{\mathbf{U}}_q = \left(\widetilde{\mathbf{H}}_q^H \widetilde{\mathbf{H}}_q\right)^{-1}$.

3) Optimal Index Selection: Then, after obtaining Q candidate channels and their corresponding transmit precoding matrices, the RIS RC configuration problem can be expressed as

$$\begin{aligned} \max_{q} \ & R_q = \sum_{k=1}^{K} \log_2 \left(1 + \frac{1}{\sigma_k^2} \left| \widetilde{\mathbf{h}}_{k,q}^H \widetilde{\mathbf{w}}_{k,q} \right|^2 \right) \\ \text{s.t.} \ & 1 \leq q \leq Q. \end{aligned} \tag{17}$$

Once the index $\hat{q}$ of the optimal training block is obtained, we get the RIS RC configuration $\hat{\mathbf{\Phi}} = \mathbf{\Phi}_{\hat{q}}$, and the corresponding transmit precoding matrix accordingly[1].

IV. Theoretical Analysis of the Proposed Scheme

In this section, we analyze the performance of the proposed environment-aware scheme by considering a single user case. We first analyze the theoretical achievable rate considering the noiseless channels in Section IV-A. Then, in Section IV-B, we analyze the influence of channel estimation errors on the proposed channel training scheme.

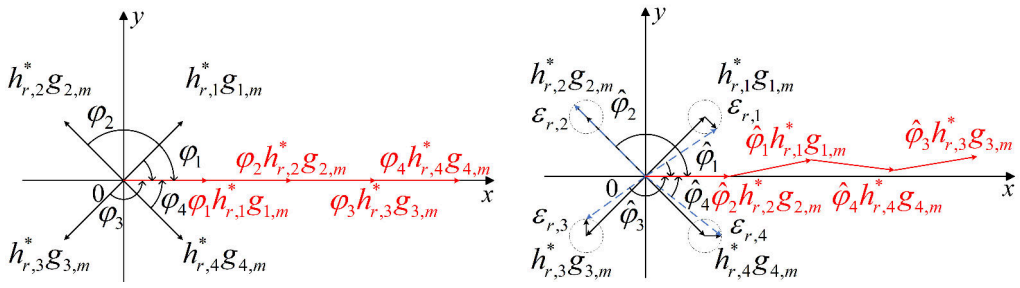
A. Perfect CSI

Firstly, we examine the scenario where there is no channel estimation error at each training block. For brevity, we assume that the direct BS-user link is blocked and the BS-RIS channel remains only the LoS component which is likely to happen in practical scenarios. Based on the above assumptions, the theoretical received power scaling law is summarized in *Proposition 1*.

Proposition 1: Assume $h_{r,n}$ following the Rician channel model with Rician factor of F_r , $n = 1, 2, \cdots, N$. For $N \gg 1$, the average signal power received by the user is given by

$$P_r = P_d \beta_r \beta_g M N \left(F_1^2 N + F_2^2 \left(\log Q + C\right) + \sqrt{\pi} F_1 F_2\right), \tag{18}$$

[1]Note that the RIS configuration is completed by selecting the optimal codeword that maximizes the sum rate. To further boost the performance, one can design appropriate codeword weighting methods to obtain better RIS configuration, which constitutes our future work.



(a) Perfect CSI (b) Imperfect CSI

Fig. 4. Conventional channel estimation and passive beamforming scheme. (Red arrow: cascaded channel including the RC configuration)

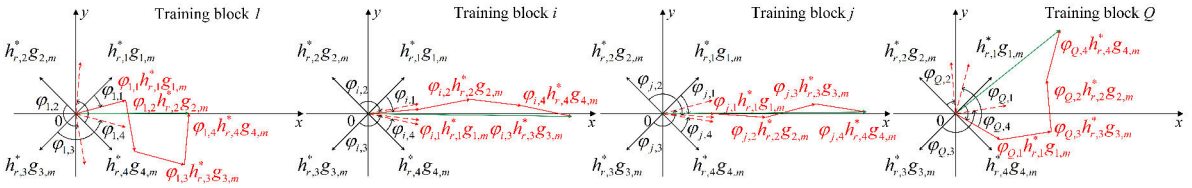
where P_d is the total transmit power of BS, Q is training overhead, $F_1 = \sqrt{\frac{F_r}{F_r+1}}$, $F_2 = \sqrt{\frac{1}{F_r+1}}$ and $C \approx 0.57722$ is the Euler-Mascheroni constant.

Proof: Please refer to Appendix A.

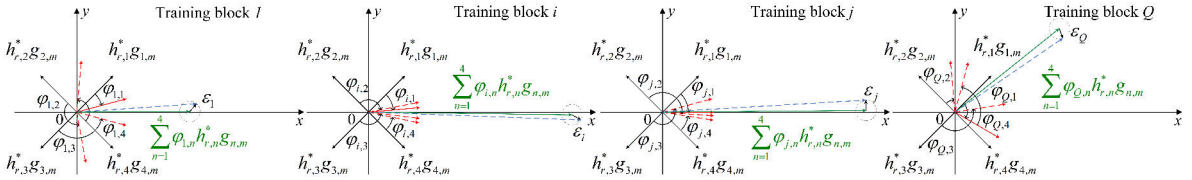
Next, we provide some useful insights into *Proposition 1* by considering four special cases:

1) As the Rician factor $F_r \to 0$, the RIS-user channel turns into the Rayleigh channel. In this case, the proposed scheme degenerates to the random phase-shift codebook scheme [22] and the received power $P_r \to P_d\beta_r\beta_g MN\,(\log Q + C)$.
2) As the Rician factor F_r approaches infinity, the RIS-user channel turns into the deterministic LoS channel, which is perfectly aligned according to the statistical CSI. In this case, we have $P_r \to P_d\beta_r\beta_g MN^2$ which characterizes the quadratic power scaling law versus the number of RIS elements [34].
3) When considering the training overhead of $Q = 1$, the environment-aware algorithm reduces to the statistical CSI-based scheme [32]. In particular, if $F_r \to 0$, we have $P_r = P_d\beta_r\beta_g MNC$, which is equivalent to a random phase shift configuration scenario. If $F_r \to +\infty$, we can achieve the power scaling law relying on the optimal RIS configuration, i.e. $P_r = P_d\beta_r\beta_g MN^2$.
4) When the training overhead reaches the maximum overhead $Q_{\max} = 2^{bN}$, we arrive at the quadratic scaling law of the average received power at the user with respect to the number of RIS elements N [22], which is comparable to the optimal RIS configuration.

As such, the proposed environment-aware codebook scheme strikes favorable tradeoffs be-



(a) Perfect CSI scenario. (Red arrow: cascaded channel including the RC configuration)



(b) Imperfect CSI scenario. (Green arrow: composite end-to-end channel; Blue dotted arrow: composite channel with error)

Fig. 5. The proposed channel training-based protocol.

tween the statistical CSI-based RIS configuration and the optimal RIS configuration method by flexibly adapting the codebook size Q.

B. Imperfect CSI

In this subsection, we analyze the theoretical achievable rate while considering the imperfect CSI. As shown in Fig. 4 and Fig. 5, we provide a scenario of four RIS elements to show the effects of the channel estimation errors.

Firstly, Fig. 4 shows the influence of channel estimation errors on conventional channel estimation and passive beamforming schemes. Observe from Fig. 4(a) that all four cascaded channels with optimal RC configuration, which are denoted by solid red arrows, are aligned when there are no channel estimation errors. In this context, the optimal achievable rate is shown in Eq. (30) of [34]. When taking into account the practical channel estimation errors, we can observe from Fig. 4(b) that the optimal phase shift associated with each RIS element is rotated, which results in the deviation from the perfect case. This results in a loss of achievable rate characterized by Eq. (29) of [23].

By contrast, the influence of channel estimation errors on the proposed environment-aware codebook scheme is shown in Fig. 5, where Fig. 5(a) represents four training blocks in the perfect CSI scenario and the corresponding cases in the imperfect CSI scenario are shown in Fig. 5(b).

Specifically, as shown in Fig. 5, $\varphi_{q,n}, q = 1, \cdots, Q, n = 1, 2, 3, 4$ represents the RC of the nth RIS element at the qth training block. They rotate the cascaded channels with the corresponding angle to get the results shown by the red arrows. In this case, the achievable rate maximization problem is equivalent to the problem

$$\max_{q \in \mathcal{Q}} Y_q = \left| \sum_{n=1}^{N} h_{r,n}^{*} \varphi_{q,n} g_{n,m} \right|^2 . \tag{19}$$

We calculate Y_q for all Q training blocks and obtain the optimal index i whose theoretical performance is analysed in *Proposition 1*.

When considering the practical channel estimation errors, it is important to note that for our channel training protocol, the effect of channel estimation errors is not reflected separately at each phase shift. Instead, it distorts the composite end-to-end channels, which is shown by the green arrow. Based on the estimated composite channels (i.e., the dotted blue arrow in Fig. 5(b)), maximizing the achievable rate problem is equivalent to

$$\max_{q \in \mathcal{Q}} \hat{Y}_q = \left| \sum_{n=1}^{N} h_{r,n}^{*} \varphi_{q,n} g_{n,m} + \varepsilon_q \right|^2 , \tag{20}$$

where $\varepsilon_q \sim \mathcal{CN}\left(0, \sigma_q^2\right)$ denotes the estimation error of the composite channel in the qth training block. It is noted that the optimal codeword index may not be correctly selected when considering channel estimation errors. In the proposed codebook scheme, the influence of the channel estimation errors is implicitly reflected in the selection of the codeword index, whose impacts are difficult to be accurately characterized. In this paper, a tight upper bound of the achievable rate is derived in *Proposition 2*.

Proposition 2: Assume $h_{r,n}$ following the Rician channel model with Rician factor of F_r , $n = 1, 2, \cdots, N$. $\varepsilon_q \sim \mathcal{CN}\left(0, \sigma_q^2\right)$, $q = 1, 2, \cdots, Q$ is the composite channel estimation error during the qth training block. For $N \gg 1$, the average signal power received by the user is given

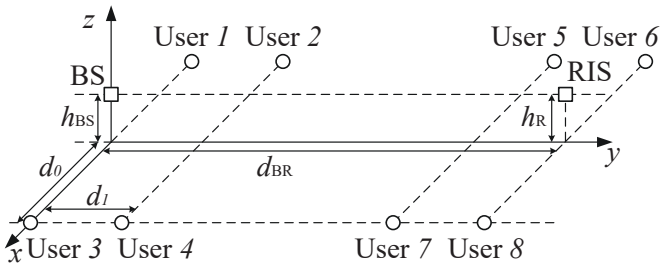


Fig. 6. Schematic of an RIS-aided multi-user communication scenario.

by

$$P_r = P_d M \beta_r \beta_g \Big(N^2 F_1^2 + N F_1 F_2 \sqrt{\pi} + N F_2^2 \frac{N + \frac{\pi}{2}(N-1)\sqrt{\frac{\beta_r \beta_g}{(N-1)\beta_r \beta_g + \sigma_q^2}}}{N + \frac{\pi}{2}\sqrt{N-1}} \left(\log Q + C \right) \Big). \tag{21}$$

Proof: Please refer to Appendix B.

V. Simulation Results

In this section, we provide numerical simulation results to validate the performance of the proposed scheme. All results are obtained by averaging 1,000 independent experiments. As shown in Fig. 6, we consider an RIS-aided multi-user system. Specifically, the antenna array at the BS is modeled by a ULA and deployed on the z-axis with antenna spacing of $d_{\mathrm{BS}} = \lambda/2$. The number of the BS antennas is set to $M = 8$. The RIS is modeled by a UPA and deployed on the y-z plane with 10×10 array structure ($N = 100$) with element spacing of $d_{\mathrm{R}} = \lambda/8$. Moreover, the Rician factor of the BS-RIS, RIS-user, and BS-user channels are $F_g = 4\,\mathrm{dB}$, $F_r = 3\,\mathrm{dB}$, and $F_d = -3\,\mathrm{dB}$, respectively. The quantization number of the discrete phase shift set is set to $b = 1$. The distance from BS to RIS, from each user to the BS-RIS line and between two adjacent users are set to $d_{\mathrm{BR}} = 100\,\mathrm{m}$, $d_0 = 2\,\mathrm{m}$ and $d_1 = 10\,\mathrm{m}$, respectively. Both the BS and RIS are situated at a height of $h_{\mathrm{BS}} = h_{\mathrm{R}} = 5\,\mathrm{m}$.

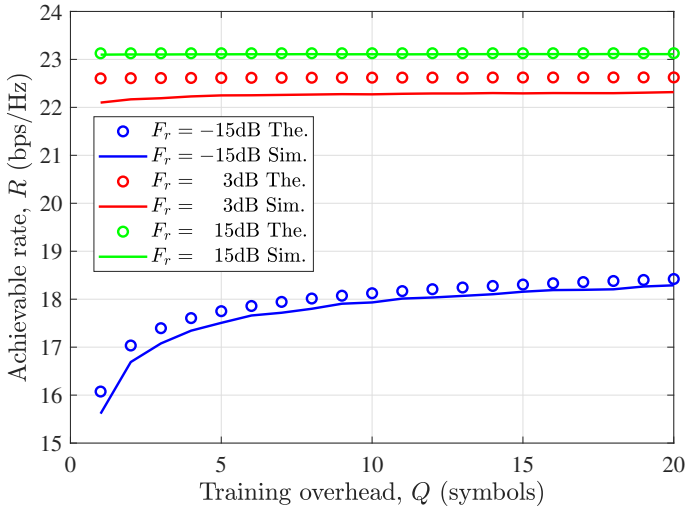


Fig. 7. Achievable rate R of the single user versus training overhead Q, where we consider perfect CSI (The.: theoretical result; Sim.: simulation result).

The path loss of each channel is modeled as [33]

$$\beta = C_0(d/d_m)^{-\alpha}, \tag{22}$$

where d is the distance of the corresponding link, $C_0 = -20\,\mathrm{dB}$ denotes the path loss of the reference distance $d_m = 1\,\mathrm{m}$ and α denotes the path loss factor.

We assume that the path loss factor of BS-RIS, RIS-user and BS-user links are $\alpha_g = 2.4$, $\alpha_r = 2.5$ and $\alpha_d = 3.5$, respectively. Moreover, we consider the transmit power at the BS is set to $P_d = 40\,\mathrm{dBm}$, the average power of the pilot signals is $P_{\text{ul}} = -23\,\mathrm{dBm}$, the average noise power at the BS and the user are $\sigma_z^2 = -110\,\mathrm{dBm}$ and $\sigma_k^2 = -90\,\mathrm{dBm}$, respectively.

Firstly, we verify the performance analysis in a single user scenario by only considering User 8 in Fig. 6. As shown in Fig. 7, we verify our analytical results in Section IV-A under different RIS-user channel conditions, where we set $F_r = -15\,\mathrm{dB}$, $3\,\mathrm{dB}$, and $15\,\mathrm{dB}$, respectively. It can be seen that the proposed codebook scheme gains an improved achievable rate as the codebook size increases. Moreover, the theoretical result offers a tight upper bound of the simulation result when confronting with diverse channel conditions.

Moreover, Fig. 8 verifies our analytical results in Section IV-B considering the channel estimation errors. It can be seen that the theoretical bound accurately characterizes the environment-

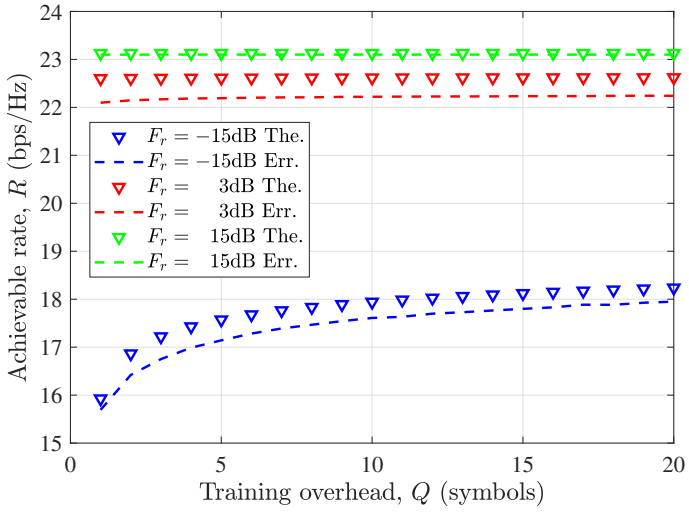


Fig. 8. Achievable rate R of the single user versus training overhead Q, where we consider imperfect CSI (Err.: simulation result with imperfect CSI).

aware codebook scheme for a high Rician factor, e.g., $F_r = 15\,\mathrm{dB}$. Besides, in the case of $F_r = 3\,\mathrm{dB}$ and $-15\,\mathrm{dB}$, the theoretical results provide a tight upper bound. Compared to Fig. 7, the performance degradation at $F_r = 15\,\mathrm{dB}$ is negligible, which implies that the codebook based on statistical CSI achieves optimal performance at high Rician factors. At $F_r = 3\,\mathrm{dB}$ and $-15\,\mathrm{dB}$, there exists moderate performance degradation in the proposed scheme, indicating strong robustness against noise.

Next, as shown in Fig. 9, we compare the sum rate versus total transmit power at BS while activating Users 6 and 8. The Rician factor of the RIS-user link is set to $F_r = 10\,\mathrm{dB}$. The training overhead is set to $Q = 100$. Note that the sum rate is improved as the transmit power increases, and exhibits a logarithmic growth trend. In addition, the proposed scheme outperforms the random codebook scheme in both the perfect and imperfect CSI scenarios. Specifically, a sum rate gain of $1.78\,\mathrm{bps/Hz}$ is observed under perfect CSI. This is because the proposed scheme generates the RIS RC codebook by leveraging the statistical CSI.

Next, we evaluate the robustness of the proposed environment-aware codebook-based scheme by considering four different setups in Fig. 10. Note that under all setups, the achievable sum rate increases with the training overhead. Besides, observe from Fig. 10 that the proposed scheme always outperforms the random codebook scheme corresponding to the training overhead $Q = 1$,

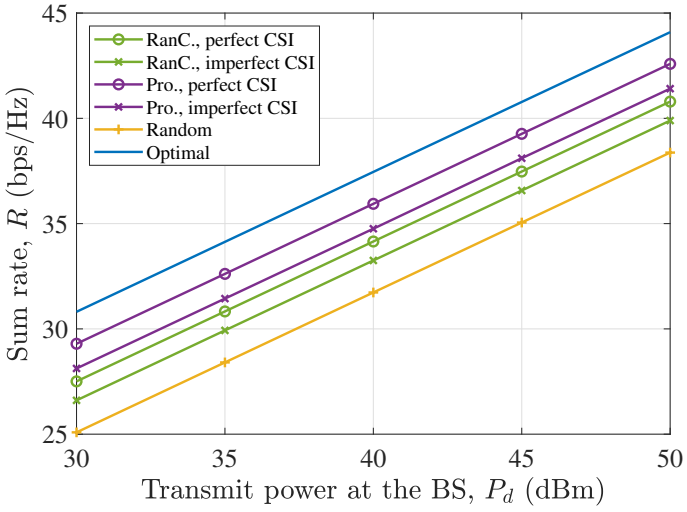
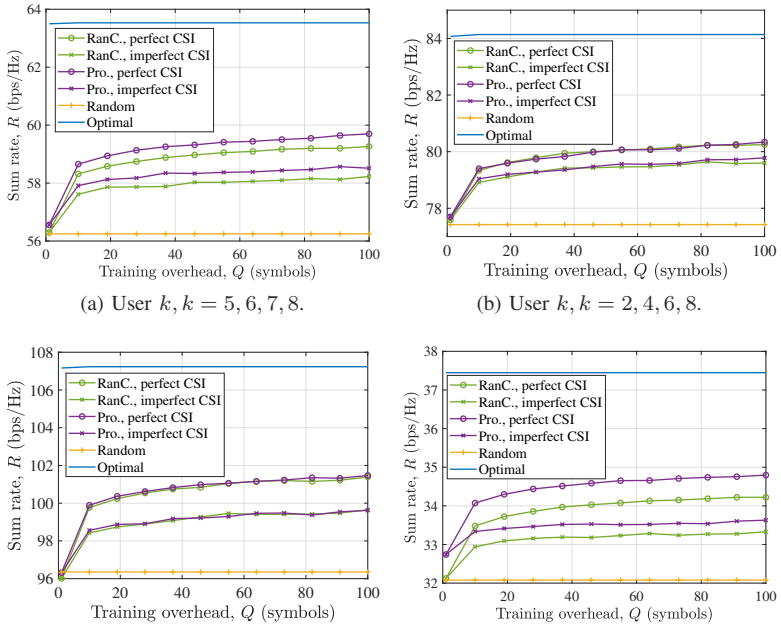


Fig. 9. Sum rate R versus transmit power P_d at the BS (RanC.: random codebook; Pro.: proposed scheme; Random: random configuration; Optimal: optimal configuration).



(a) User $k, k = 5, 6, 7, 8$. (b) User $k, k = 2, 4, 6, 8$.

(c) User $k, k = 2, 4, 5, 6, 7, 8$. (d) User $k, k = 6, 8$.

Fig. 10. Sum rate R versus training overhead Q.

due to the fact that the proposed scheme utilizes the statistical CSI to design the phase shift codebook. Further comparing Figs. 10(a)-10(c) that activating more users results in an improved sum rate, thanks to the multi-user multiplexing gain. For instance, the sum rate increases by $24.90\,\mathrm{bps/Hz}$ from activating users 6 and 8 to activating users $5, 6, 7$ and 8. Furthermore, we

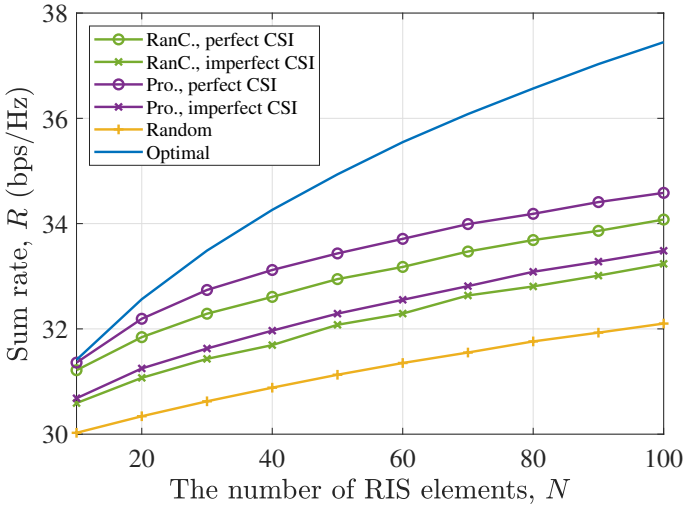


Fig. 11. Sum rate R versus the number of RIS elements N.

note that the advantage of the proposed scheme over the random codebook scheme is more significant in Figs. 10(a) and 10(d). Both these two cases correspond to activating users near the RIS. Moreover, Fig. 10 shows that the influence caused by the channel estimation errors becomes severe as the training overhead increases, which is consistent with our analysis accounting for the imperfect CSI in Section IV-B.

Next, Fig. 11 compares the sum rate versus the number of RIS elements, considering users 6 and 8 and setting the training overhead to $Q = 50$. It can be observed that the proposed scheme outperforms the random codebook scheme under all setups. Besides, as the number of RIS elements increases from $N = 10$ to $N = 100$, the proposed scheme results in a more significant sum rate improvement with diminishing return, which is due to the fact that a larger number of reflecting elements could reap more radiating energy by coherently superimposing all cascaded links.

Finally, Fig. 12 evaluates the effective sum rate versus the channel coherence time, where we only activate users 6 and 8 and consider four different training overhead scenarios. Here, the effective sum rate is defined by

$$R_e = \frac{T_c - \tau}{T_c} \mathbb{E}\left\{ \sum_{k=1}^{K} \log_2 \left(1 + \frac{\left| \mathbf{h}_k^H \mathbf{w}_k \right|^2}{\sum_{l \neq k}^{K} \left| \mathbf{h}_k^H \mathbf{w}_l \right|^2 + \sigma_k^2} \right) \right\}, \tag{23}$$

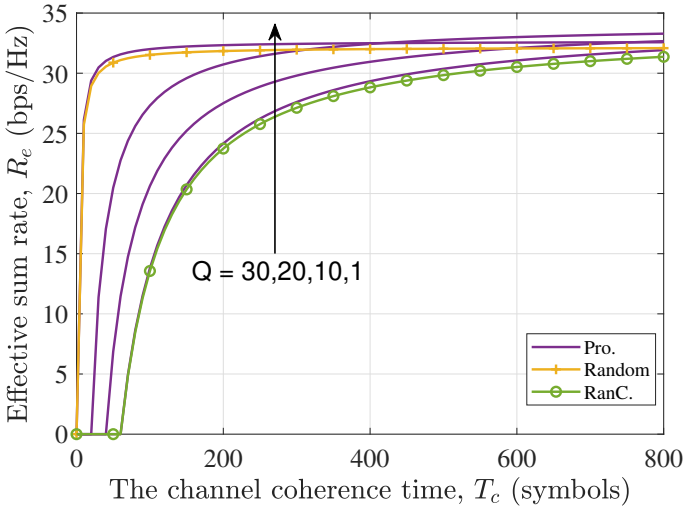


Fig. 12. The effective sum rate R_e versus the channel coherence time T_c.

where T_c is the channel coherence time and τ is the pilot overhead. It can be seen that the proposed scheme can flexibly adapt the pilot overhead in the face of different values of channel coherence time. Specifically, for a rapidly time-varying channel (e.g., $T_c \leq 200$), the effective sum rate of the proposed scheme with training overhead $Q = 1$ attains the best performance. However, as the channel coherence time becomes longer, the increased training overhead can lead to a higher effective sum rate. Therefore, based on the specific coherence time, the proposed scheme can flexibly adjust the training overhead, thus maximizing the effective sum rate.

VI. Conclusion

In this paper, we have proposed a channel training-based protocol for RIS-assisted MU-MISO systems, where an environment-aware RC codebook is designed. Specifically, during the off-line stage, the proposed scheme generates a set of virtual channels based on the statistical CSI and obtains an environment-aware codebook according to the off-line AO algorithm. Then, during the on-line stage, we have configured the RIS based on the environment-aware codebook and have directly estimated the composite end-to-end channels. Subsequently, we have performed the ZF precoding design at the BS to obtain candidate channels. Finally, the optimal codeword resulting in the highest sum rate has been adopted to configure the RIS for assisting in the data transmission. Furthermore, we have analyzed the performance of the proposed scheme

accounting for both the perfect and the imperfect CSI scenarios and have evaluated the achievable rate of the environment-aware codebook scheme through simulation results. It has been shown that the proposed scheme has better performance than traditional codebook schemes, and can strike a favorable trade-off between performance and the training overhead. We highlight that the proposed scheme can be applied to a wider range of wireless systems including cell-free massive MIMO systems and OFDM systems by leveraging the statistical CSI therein [19], [46], [52], [53].

APPENDIX A
PROOF OF PROPOSITION 1

By applying the assumptions of *Proposition 1*, let $\mathcal{Q} = \{1, 2, \cdots, Q\}$, the average received power P_r at the single user with codebook based RC configuration can be expressed as

$$P_r = P_d \mathbb{E}\left\{ \max_{q \in \mathcal{Q}} \|\mathbf{h}_r^H \mathbf{\Phi}_q \mathbf{G}\|^2 \right\}. \tag{24}$$

Due to the fact that the maximum value of the sum does not exceed the sum of the maximum values, (24) can be further written as

$$\begin{aligned} P_r &= P_d \mathbb{E}\left\{ \max_{q \in \mathcal{Q}} \left\| \sum_{n=1}^{N} h_{r,n}^* \varphi_{q,n} \mathbf{g}_n^T \right\|^2 \right\} \\ &\leq P_d \mathbb{E}\left\{ \sum_{m=1}^{M} \max_{q \in \mathcal{Q}} \left| \sum_{n=1}^{N} h_{r,n}^* \varphi_{q,n} g_{n,m} \right|^2 \right\} \\ &= P_d \beta_r \beta_g M \mathbb{E}\left\{ \max_{q \in \mathcal{Q}} \left| \sum_{n=1}^{N} \overline{h}_{r,n}^* \varphi_{q,n} \overline{g}_{n,m} \right|^2 \right\}, \end{aligned} \tag{25}$$

where $\mathbf{g}_n^T$ is the nth row of $\mathbf{G}$ and '$\leq$' reduces to '=' if and only if $\text{rank}(\mathbf{G}) = 1$; $h_{r,n}$ and $g_{n,m}$ are the nth entry of $\mathbf{h}_r$ and $\mathbf{g}_m$, respectively; $\overline{h}_{r,n}^*$ and $\overline{g}_{n,m}$ denote their normalized results, respectively. $\varphi_{q,n}$ is the nth entry on the diagonal of $\mathbf{\Phi}_q$.

Since we have $\overline{h}_{r,n}^* = F_1\left(h_{r,n}^{\text{LoS}}\right)^* + F_2\left(h_{r,n}^{\text{NLoS}}\right)^*$ and $\overline{g}_{n,m} = g_{n,m}^{\text{LoS}}$, $\left|\sum_{n=1}^{N} \overline{h}_{r,n}^* \varphi_{q,n} \overline{g}_{n,m}\right|^2$ can be

further written as

$$\begin{aligned}
&\left|\sum_{n=1}^{N}\overline{h}_{r,n}^{*}\varphi_{q,n}\overline{g}_{n,m}\right|^2\\
=&\left|\sum_{n=1}^{N}\left(F_1\left(h_{r,n}^{\mathrm{LoS}}\right)^{*}+F_2\left(h_{r,n}^{\mathrm{NLoS}}\right)^{*}\right)\varphi_{q,n}g_{n,m}^{\mathrm{LoS}}\right|^2\\
=&\left|\sum_{n=1}^{N}F_1\left(h_{r,n}^{\mathrm{LoS}}\right)^{*}\varphi_{q,n}g_{n,m}^{\mathrm{LoS}}\right|^2+\left|\sum_{n=1}^{N}F_2\left(h_{r,n}^{\mathrm{NLoS}}\right)^{*}\varphi_{q,n}g_{n,m}^{\mathrm{LoS}}\right|^2\\
&+2\Re\left\{\left(\sum_{n=1}^{N}F_1\left(h_{r,n}^{\mathrm{LoS}}\right)^{*}\varphi_{q,n}g_{n,m}^{\mathrm{LoS}}\right)^{*}\right.\\
&\left.\times\left(\sum_{n=1}^{N}F_2\left(h_{r,n}^{\mathrm{NLoS}}\right)^{*}\varphi_{q,n}g_{n,m}^{\mathrm{LoS}}\right)\right\}. \qquad (26)
\end{aligned}$$

Note that we adopt the environment-aware scheme relying on the statistical CSI. In each channel training block, we generate the NLoS component of the RIS-user channel and configure the phase shift of the nth RIS element as

$$\theta_{q,n}=\angle\left(\sqrt{F_r}h_{r,n}^{\mathrm{LoS}}+\tilde{h}_{r,q,n}^{\mathrm{NLoS}}\right)-\angle\left(g_{n,m}^{\mathrm{LoS}}\right), \qquad (27)$$

where $\tilde{h}_{r,q,n}^{\mathrm{NLoS}}$ is the random NLoS component generated off-line. Thus when considering the Rayleigh fading in the proposed scheme, it is equivalent to adopting a random phase-shift configuration codebook.

Then, we consider the three terms of (26) separately. Specifically, for the first entry of (26), the LoS component of multiple reflected channels is largely aligned thus it can be expressed as

$$\begin{aligned}
&\mathbb{E}\left\{\max_{q\in\mathcal{Q}}\left|\sum_{n=1}^{N}F_1\left(h_{r,n}^{\mathrm{LoS}}\right)^{*}\varphi_{q,n}g_{n,m}^{\mathrm{LoS}}\right|^2\right\}\\
&=F_1^2\left|\sum_{n=1}^{N}\left|\left(h_{r,n}^{\mathrm{LoS}}\right)^{*}\right|\left|g_{n,m}^{\mathrm{LoS}}\right|\right|^2=F_1^2N^2. \qquad (28)
\end{aligned}$$

The other two entries of (26) are related to the NLoS component, where we can obtain $\sum_{n=1}^{N}\varphi_{q,n}\left(h_{r,n}^{\mathrm{NLoS}}\right)^{*}g_{n,m}^{\mathrm{LoS}}\sim\mathcal{CN}\left(0,N\right)$ as $N\rightarrow\infty$ based on Lindeberg-Levy central limit theorem [34].

Specifically, the second entry reflects the effects on the NLoS component of the channel. According to *Lemma 1* in [22], we have

$$\max_{q\in\mathcal{Q}}\left|\sum_{n=1}^{N}\varphi_{q,n}\left(h_{r,n}^{\text{NLoS}}\right)^{*}g_{n,m}^{\text{LoS}}\right|^{2}\overset{d}{=}N\sum_{j=1}^{Q}\frac{1}{Q-j+1}\rho_{j}, \tag{29}$$

where ρ_j are i.i.d. standard exponential random variables with a rate parameter of 1. Thus we have $\mathbb{E}\{\rho_j\}=1$ and it can be obtained that

$$\begin{aligned}&\mathbb{E}\left\{\max_{q\in\mathcal{Q}}\left|\sum_{n=1}^{N}F_2\left(h_{r,n}^{\text{NLoS}}\right)^{*}\varphi_{q,n}g_{n,m}^{\text{LoS}}\right|^{2}\right\}\\ =&F_2^2\mathbb{E}\left\{N\sum_{j=1}^{Q}\frac{1}{Q-j+1}\rho_j\right\}\\ =&F_2^2N\left(\log Q+C\right).\end{aligned} \tag{30}$$

Since we have $\mathbb{E}\left\{\sum_{n=1}^{N}\varphi_{q,n}\left(h_{r,n}^{\text{NLoS}}\right)^{*}g_{n,m}^{\text{LoS}}\right\}=0$, the third entry of (26) can be further derived as

$$\begin{aligned}&\mathbb{E}\left\{\max_{q\in\mathcal{Q}}2\Re\left\{\left(\sum_{n=1}^{N}F_1\left(h_{r,n}^{\text{LoS}}\right)^{*}\varphi_{q,n}g_{n,m}^{\text{LoS}}\right)^{*}\right.\right.\\ &\left.\left.\times\left(\sum_{n=1}^{N}F_2\left(h_{r,n}^{\text{NLoS}}\right)^{*}\varphi_{q,n}g_{n,m}^{\text{LoS}}\right)\right\}\right\}\\ =&2F_1F_2\Re\left\{\mathbb{E}\left\{\max_{q\in\mathcal{Q}}\left\{\sum_{n=1}^{N}\left|\varphi_{q,n}\right|^2h_{r,n}^{\text{LoS}}\left(h_{r,n}^{\text{NLoS}}\right)^{*}\left|g_{n,m}^{\text{LoS}}\right|^2+\right.\right.\right.\\ &\left.\left.\left.\left(\sum_{i=1}^{N}\varphi_{q,i}\left(h_{r,i}^{\text{NLoS}}\right)^{*}g_{i,m}^{\text{LoS}}\right)\left(\sum_{j\neq i}\varphi_{q,j}^{*}h_{r,j}^{\text{LoS}}(g_{j,m}^{\text{LoS}})^{*}\right)\right\}\right\}\right\}\\ \overset{(a)}{=}&2F_1F_2\Re\left\{\mathbb{E}\left\{\sum_{n=1}^{N}h_{r,n}^{\text{LoS}}\left(h_{r,n}^{\text{NLoS}}\right)^{*}\right\}\right\}\\ \overset{(b)}{<}&2F_1F_2\sum_{n=1}^{N}\left(\left|h_{r,n}^{\text{LoS}}\right|\mathbb{E}\left\{\left|(h_{r,n}^{\text{NLoS}})^{*}\right|\right\}\right)\\ \overset{(c)}{=}&\sqrt{\pi}F_1F_2N,\end{aligned} \tag{31}$$

where (a) holds because we have $\mathbb{E}\left\{\sum_{i=1}^{N}\varphi_{q,i}\left(h_{r,i}^{\text{NLoS}}\right)^{*}g_{i,m}^{\text{LoS}}\right\}=0$, $\left|g_{n,m}^{\text{LoS}}\right|=1$ and $|\varphi_{q,n}|=1$;

(b) holds as we have $\Re\left\{\mathbb{E}\left\{\sum_{n=1}^{N} h_{r,n}^{\mathrm{LoS}}\left(h_{r,n}^{\mathrm{NLoS}}\right)^{*}\right\}\right\} < \sum_{n=1}^{N}\mathbb{E}\left\{\Re\left\{h_{r,n}^{\mathrm{LoS}}\right\}\right\}\mathbb{E}\left\{\Re\left\{\left(h_{r,n}^{\mathrm{NLoS}}\right)^{*}\right\}\right\}$, $\Re\left\{h_{r,n}^{\mathrm{LoS}}\right\} \le \left|h_{r,n}^{\mathrm{LoS}}\right|$ and $\Re\left\{\left(h_{r,n}^{\mathrm{NLoS}}\right)^{*}\right\} \le \left|(h_{r,n}^{\mathrm{NLoS}})^{*}\right|$; Moreover, equality (c) holds due to the fact that $\left|\left(h_{r,n}^{\mathrm{NLoS}}\right)^{*}\right|$ follows Rayleigh distribution with mean value of $\sqrt{\pi}/2$.

Substituting (28), (30) and (31) into (26), the proof is completed. ■

APPENDIX B
PROOF OF PROPOSITION 2

Similar to (26), the average received power P_r of the single user when considering channel estimation errors is given by

$$\begin{aligned} P_r = P_d\beta_r\beta_g M\mathbb{E}\Bigg\{ & \left|\sum_{n=1}^{N} F_1\left(h_{r,n}^{\mathrm{LoS}}\right)^{*}\varphi_{\hat{q},n}g_{n,m}^{\mathrm{LoS}}\right|^2 \\ & + \left|\sum_{n=1}^{N} F_2\left(h_{r,n}^{\mathrm{NLoS}}\right)^{*}\varphi_{\hat{q},n}g_{n,m}^{\mathrm{LoS}}\right|^2 \\ & + 2\Re\Bigg\{\left(\sum_{n=1}^{N} F_1\left(h_{r,n}^{\mathrm{LoS}}\right)^{*}\varphi_{\hat{q},n}g_{n,m}^{\mathrm{LoS}}\right)^{*} \\ & \times\left(\sum_{n=1}^{N} F_2\left(h_{r,n}^{\mathrm{NLoS}}\right)^{*}\varphi_{\hat{q},n}g_{n,m}^{\mathrm{LoS}}\right)\Bigg\}\Bigg\}, \end{aligned} \tag{32}$$

where $\varphi_{\hat{q},n}$ is the RC with selected index $\hat{q}$ for the nth RIS element in the presence of channel estimation errors, which is obtained by

$$\varphi_{\hat{q},n} = \arg\max_{q\in\mathcal{Q}}\left|\sum_{i\neq n}^{N} h_{r,i}^{*}\varphi_{q,i}g_{i,m} + h_{r,n}^{*}\varphi_{q,n}g_{n,m} + \varepsilon_q\right|^2, \tag{33}$$

where $\varphi_{q,n}$ represents the RC of the nth RIS element at the qth training block, and $\varphi_{q,i}, i\neq n$ represent the fixed $(N-1)$ RCs when optimizing $\varphi_{q,n}$. $\varepsilon_q \sim \mathcal{CN}\left(0,\sigma_q^2\right)$ is the composite channel estimation error in the qth training block.

Then, as illustrated in Fig. 5, we select the optimal RC configuration maximizing the sum rate in the imperfect CSI scenario. Since the codewords are obtained based on the statistical CSI, the first entry of (32) is equal to that without channel estimation errors. Moreover, as we have $\mathbb{E}\left\{\sum_{i=1}^{N}\left(h_{r,n}^{\mathrm{NLoS}}\right)^{*}\varphi_{\hat{q},i}g_{i,m}^{\mathrm{LoS}}\right\} = 0$, the result of the third part remains the same with that considering perfect CSI, i.e., (31).

Under imperfect CSI conditions, the second entry of (32) still follows an exponential distribution at each training block. However, the Qth order statistics is a scaling version of that in (32). Let u denote the scaling factor. Specifically, we first consider the effect of the channel estimation errors on a single RC, keeping the remaining $(N-1)$ terms fixed, i.e., $\sum_{i\neq n}^{N}\sqrt{\beta_r}(h_{r,i}^{\text{NLoS}})^*\varphi_{q,i}\sqrt{\beta_g}g_{i,m}^{\text{LoS}} \sim \mathcal{CN}\left(0,(N-1)\beta_r\beta_g\right)$. Next, we derive the scaling factor to characterize the influence of the channel estimation errors.

Let $h_{c,n}^* = \sqrt{\beta_r}(h_{r,n}^{\text{NLoS}})^*\sqrt{\beta_g}g_{n,m}^{\text{LoS}}$ represent the NLoS component of the cascaded channel spanning from the user to the BS through the nth RIS element. Hence, by solving (19), it is straightforward to obtain the optimal RC for the nth RIS element $\bar{\varphi}_{q,n} = \frac{h_{c,n}}{\left|h_{c,n}^*\right|}\frac{\sum_{i\neq n}^{N}h_{c,i}^*\varphi_{q,i}}{\left|\sum_{i\neq n}^{N}h_{c,i}^*\varphi_{q,i}\right|}$, and the second term in (32) can be simplified to

$$\begin{aligned} u_o &\triangleq \left|\sum_{i\neq n}^{N}h_{c,i}^*\varphi_{q,i} + h_{c,n}^*\bar{\varphi}_{q,n}\right|^2 \\ &= \left|\sum_{i\neq n}^{N}h_{c,i}^*\varphi_{q,i}\right|^2 + |h_{c,n}|^2 + 2\Re\left\{\left|\sum_{i\neq n}^{N}h_{c,i}\varphi_{q,i}^*\right|\left|h_{c,n}^*\right|\right\}. \end{aligned} \tag{34}$$

Moreover, we obtain the optimal RC under imperfect CSI by solving (20), i.e., $\hat{\varphi}_{q,n} = \frac{h_{c,n}}{\left|h_{c,n}^*\right|}\frac{\sum_{i\neq n}^{N}h_{c,i}^*\varphi_{q,i}+\varepsilon_q}{\left|\sum_{i\neq n}^{N}h_{c,i}^*\varphi_{q,i}+\varepsilon_q\right|}$, we have

$$\begin{aligned} u_e &\triangleq \left|\sum_{i\neq n}^{N}h_{c,i}^*\varphi_{q,i} + h_{c,n}^*\hat{\varphi}_{q,n}\right|^2 \\ &= \left(\left|\sum_{i\neq n}^{N}h_{c,i}^*\varphi_{q,i}\right|^2 + \left|h_{c,n}^*\right|^2\right. \\ &\quad \left.+2\Re\left\{\sum_{i\neq n}^{N}h_{c,i}\varphi_{q,i}^*\left|h_{c,n}^*\right|\frac{\sum_{i\neq n}^{N}h_{c,i}^*\varphi_{q,i}+\varepsilon_q}{\left|\sum_{i\neq n}^{N}h_{c,i}^*\varphi_{q,i}+\varepsilon_q\right|}\right\}\right). \end{aligned} \tag{35}$$

The expectation of the third entry in (35) can be expressed as

$$\begin{aligned}
&\mathbb{E}\left\{2\Re\left\{\sum_{i\neq n}^{N} h_{c,i}\varphi_{q,i}^{*}\left|h_{c,n}^{*}\right|\frac{\sum_{i\neq n}^{N} h_{c,i}^{*}\varphi_{q,i}+\varepsilon_{q}}{\left|\sum_{i\neq n}^{N} h_{c,i}^{*}\varphi_{q,i}+\varepsilon_{q}\right|}\right\}\right\} \\
&=2\mathbb{E}\left\{\left|h_{c,n}^{*}\right|\Re\left\{\sum_{i\neq n}^{N} h_{c,i}\varphi_{q,i}^{*}\frac{\sum_{i\neq n}^{N} h_{c,i}^{*}\varphi_{q,i}+\varepsilon_{q}}{\left|\sum_{i\neq n}^{N} h_{c,i}^{*}\varphi_{q,i}+\varepsilon_{q}\right|}\right\}\right\}. \qquad (36)
\end{aligned}$$

According to the assumptions of $h_{c,n}^{*}\sim\mathcal{CN}\left(0,\beta_r\beta_g\right), n=1,2,\cdots,N$, $\sum_{i\neq n}^{N} h_{c,i}\varphi_{q,i}^{*}\sim\mathcal{CN}\left(0,(N-1)\beta_r\beta_g\right)$, $\varepsilon_q\sim\mathcal{CN}\left(0,\sigma_q^2\right), q=1,2,\cdots,Q$, we have

$$\begin{aligned}
&\mathbb{E}\left\{\left|\sum_{i\neq n}^{N} h_{c,i}^{*}\varphi_{q,i}\right|^{2}\right\}=(N-1)\beta_r\beta_g, \\
&\mathbb{E}\left\{\left|h_{c,n}^{*}\right|^{2}\right\}=\beta_r\beta_g,\ \mathbb{E}\left\{\left|h_{c,n}^{*}\right|\right\}=\frac{\sqrt{\pi}}{2}\sqrt{\beta_r\beta_g}, \\
&\mathbb{E}\left\{\Re\left\{\left|\sum_{i\neq n}^{N} h_{c,i}\varphi_{q,i}^{*}\right|\left|h_{c,n}^{*}\right|\right\}\right\}=\frac{\pi}{4}\sqrt{N-1}\beta_r\beta_g, \\
&\mathbb{E}\left\{\Re\left\{\sum_{i\neq n}^{N} h_{c,i}\varphi_{q,i}^{*}\frac{\sum_{i\neq n}^{N} h_{c,i}^{*}\varphi_{q,i}+\varepsilon_{q}}{\left|\sum_{i\neq n}^{N} h_{c,i}^{*}\varphi_{q,i}+\varepsilon_{q}\right|}\right\}\right\} \\
&=\frac{\sqrt{\pi}(N-1)\beta_r\beta_g}{2\sqrt{(N-1)\beta_r\beta_g+\sigma_q^2}}. \qquad (37)
\end{aligned}$$

As a result, the scaling factor is obtained by

$$\begin{aligned}
u&\triangleq\frac{\mathbb{E}\left\{u_e\right\}}{\mathbb{E}\left\{u_o\right\}} \\
&=\frac{N+\frac{\pi}{2}(N-1)\sqrt{\frac{\beta_r\beta_g}{(N-1)\beta_r\beta_g+\sigma_q^2}}}{N+\frac{\pi}{2}\sqrt{N-1}}. \qquad (38)
\end{aligned}$$

Applying (38) to the second entry of (32), we arrive at

$$\begin{aligned}
&\mathbb{E}\left\{\left|\sum_{n=1}^{N} F_2\left(h_{r,n}^{\mathrm{NLoS}}\right)^* \varphi_{\hat{q},n} g_{n,m}^{\mathrm{LoS}}\right|^2\right\} \\
&< F_2^2 u \mathbb{E}\left\{\max_{q\in\mathcal{Q}}\left|\sum_{n=1}^{N}\left(h_{r,n}^{\mathrm{NLoS}}\right)^* \varphi_{q,n} g_{n,m}^{\mathrm{LoS}}\right|^2\right\} \\
&= F_2^2 \frac{N+\frac{\pi}{2}(N-1)\sqrt{\frac{\beta_r\beta_g}{(N-1)\beta_r\beta_g+\sigma_q^2}}}{N+\frac{\pi}{2}\sqrt{N-1}} N(\log Q + C). \qquad (39)
\end{aligned}$$

Combining the three entries in (32), the proof is completed. ■

REFERENCES

[1] Z. Yu, J. An, L. Gan, and C. Yuen, "Environment-aware codebook for RIS-assisted MU-MISO communications: Implementation and performance analysis," *arXiv preprint arXiv:2404.00265*, 2024.

[2] T. Cui, S. Jin, J. Zhang *et al.*, "Research report on reconfigurable intelligent surface (RIS)," *IMT-2030 (6G) Promotion Group*, Sep. 2021.

[3] Y. Liu, X. Liu, X. Mu, T. Hou, J. Xu, M. Di Renzo, and N. Al-Dhahir, "Reconfigurable intelligent surfaces: Principles and opportunities," *IEEE Commun. Surv. Tutor.*, vol. 23, no. 3, pp. 1546–1577, May. 2021.

[4] E. Basar, M. Di Renzo, J. De Rosny, M. Debbah, M.-S. Alouini, and R. Zhang, "Wireless communications through reconfigurable intelligent surfaces," *IEEE Access*, vol. 7, pp. 116 753–116 773, Aug. 2019.

[5] F. Boccardi, R. W. Heath, A. Lozano, T. L. Marzetta, and P. Popovski, "Five disruptive technology directions for 5G," *IEEE Commun. Mag.*, vol. 52, no. 2, pp. 74–80, Feb. 2014.

[6] Q. Wu and R. Zhang, "Towards smart and reconfigurable environment: Intelligent reflecting surface aided wireless network," *IEEE Commun. Mag.*, vol. 58, no. 1, pp. 106–112, Aug. 2019.

[7] E. Björnson, Ö. Özdogan, and E. G. Larsson, "Intelligent reflecting surface versus decode-and-forward: How large surfaces are needed to beat relaying?" *IEEE Wireless Commun. Lett.*, vol. 9, no. 2, pp. 244–248, Nov. 2019.

[8] E. Shi, J. Zhang, H. Du, B. Ai, C. Yuen, D. Niyato, K. B. Letaief *et al.*, "RIS-aided cell-free massive MIMO systems for 6G: Fundamentals, system design, and applications," *arXiv preprint arXiv:2310.00263*, 2023.

[9] M. Di Renzo, A. Zappone, M. Debbah, M.-S. Alouini, C. Yuen, J. De Rosny, and S. Tretyakov, "Smart radio environments empowered by reconfigurable intelligent surfaces: How it works, state of research, and the road ahead," *IEEE J. Sel. Areas Commun.*, vol. 38, no. 11, pp. 2450–2525, Apr. 2020.

[10] S. Li, B. Duo, M. Di Renzo, M. Tao, and X. Yuan, "Robust secure UAV communications with the aid of reconfigurable intelligent surfaces," *IEEE Trans. Wireless Commun.*, vol. 20, no. 10, pp. 6402–6417, Apr. 2021.

[11] W. Tang, J. Y. Dai, M. Z. Chen, K.-K. Wong, X. Li, X. Zhao, S. Jin, Q. Cheng, and T. J. Cui, "MIMO transmission through reconfigurable intelligent surface: System design, analysis, and implementation," *IEEE J. Sel. Areas Commun.*, vol. 38, no. 11, pp. 2683–2699, Nov. 2020.

[12] S. Kayraklık, I. Yildirim, Y. Gevez, E. Basar, and A. Görçin, "Indoor coverage enhancement for RIS-assisted communication systems: Practical measurements and efficient grouping," in *Proc. 2023 IEEE Int. Conf. Commun. (ICC)*, May. 2023, pp. 1–6.

[13] J. An, C. Yuen, C. Xu, H. Li, D. W. K. Ng, M. D. Renzo, M. Debbah, and L. Hanzo, "Stacked intelligent metasurface-aided MIMO transceiver design," *IEEE Wireless Commun.*, pp. 1–9, 2024, Early Access.

[14] J. An, C. Xu, D. W. K. Ng, G. C. Alexandropoulos, C. Huang, C. Yuen, and L. Hanzo, "Stacked intelligent metasurfaces for efficient holographic MIMO communications in 6G," *IEEE J. Sel. Areas Commun.*, Aug. 2023.

[15] J. An, M. Di Renzo, M. Debbah, H. V. Poor, and C. Yuen, "Stacked intelligent metasurfaces for multiuser downlink beamforming in the wave domain," *arXiv preprint arXiv:2309.02687*, May. 2023.

[16] J. An, C. Yuen, C. Huang, M. Debbah, H. Vincent Poor, and L. Hanzo, "A tutorial on holographic MIMO communications—part I: Channel modeling and channel estimation," *IEEE Commun. Lett.*, vol. 27, no. 7, pp. 1664–1668, May. 2023.

[17] S. Zhang and R. Zhang, "Capacity characterization for intelligent reflecting surface aided MIMO communication," *IEEE J. Sel. Areas Commun.*, vol. 38, no. 8, pp. 1823–1838, Aug. 2020.

[18] C. Huang, A. Zappone, G. C. Alexandropoulos, M. Debbah, and C. Yuen, "Reconfigurable intelligent surfaces for energy efficiency in wireless communication," *IEEE Trans. Wireless Commun.*, vol. 18, no. 8, pp. 4157–4170, Jun. 2019.

[19] E. Shi, J. Zhang, R. He, H. Jiao, Z. Wang, B. Ai, and D. W. K. Ng, "Spatially correlated reconfigurable intelligent surfaces-aided cell-free massive MIMO systems," *IEEE Trans. Veh. Technol.*, vol. 71, no. 8, pp. 9073–9077, Aug. 2022.

[20] E. Shi, J. Zhang, D. W. K. Ng, and B. Ai, "Uplink performance of RIS-aided cell-free massive MIMO system with electromagnetic interference," *IEEE J. Sel. Areas Commun.*, vol. 41, no. 8, pp. 2431–2445, Jun. 2023.

[21] C. You, B. Zheng, and R. Zhang, "Channel estimation and passive beamforming for intelligent reflecting surface: Discrete phase shift and progressive refinement," *IEEE J. Sel. Areas Commun.*, vol. 38, no. 11, pp. 2604–2620, Mar. 2020.

[22] J. An and L. Gan, "The low-complexity design and optimal training overhead for IRS-assisted MISO systems," *IEEE Wireless Commun. Lett.*, vol. 10, no. 8, pp. 1820–1824, May. 2021.

[23] J. An, C. Xu, L. Wang, Y. Liu, L. Gan, and L. Hanzo, "Joint training of the superimposed direct and reflected links in reconfigurable intelligent surface assisted multiuser communications," *IEEE Trans. Green Commun. Netw.*, vol. 6, no. 2, pp. 739–754, Jun. 2022.

[24] Z. Wang, L. Liu, and S. Cui, "Channel estimation for intelligent reflecting surface assisted multiuser communications: Framework, algorithms, and analysis," *IEEE Trans. Wireless Commun.*, vol. 19, no. 10, pp. 6607–6620, Jun. 2020.

[25] D. Mishra and H. Johansson, "Channel estimation and low-complexity beamforming design for passive intelligent surface assisted MISO wireless energy transfer," in *Proc. IEEE Int. Conf. on Acoust., Speech and Signal Process. (ICASSP)*. IEEE, Apr. 2019, pp. 4659–4663.

[26] C. Xu, J. An, T. Bai, S. Sugiura, R. G. Maunder, Z. Wang, L.-L. Yang, and L. Hanzo, "Channel estimation for reconfigurable intelligent surface assisted high-mobility wireless systems," *IEEE Trans. Veh. Technol.*, vol. 72, no. 1, pp. 718–734, Jan. 2023.

[27] X. Wei, D. Shen, and L. Dai, "Channel estimation for RIS assisted wireless communications—part II: An improved solution based on double-structured sparsity," *IEEE Commun. Lett.*, vol. 25, no. 5, pp. 1403–1407, May. 2021.

[28] Y. Guo, P. Sun, Z. Yuan, C. Huang, Q. Guo, Z. Wang, and C. Yuen, "Efficient channel estimation for RIS-aided MIMO communications with unitary approximate message passing," *IEEE Trans. Wireless Commun.*, Feb. 2023.

[29] J. Chen, Y.-C. Liang, H. V. Cheng, and W. Yu, "Channel estimation for reconfigurable intelligent surface aided multi-user mmWave MIMO systems," *IEEE Trans. Wireless Commun.*, Oct. 2023.

[30] W. Xu, J. An, Y. Xu, C. Huang, L. Gan, and C. Yuen, "Time-varying channel prediction for RIS-assisted MU-MISO networks via deep learning," *IEEE Trans. Cogn. Commun. Netw.*, vol. 8, no. 4, pp. 1802–1815, Dec. 2022.

[31] J. An, H. Li, D. W. K. Ng, and C. Yuen, "Fundamental detection probability vs. achievable rate tradeoff in integrated sensing and communication systems," *IEEE Trans. Wireless Commun.*, vol. 22, no. 12, pp. 9835–9853, Dec. 2023.

[32] Y. Han, W. Tang, S. Jin, C.-K. Wen, and X. Ma, "Large intelligent surface-assisted wireless communication exploiting statistical CSI," *IEEE Trans. Veh. Technol.*, vol. 68, no. 8, pp. 8238–8242, Aug. 2019.

[33] J. An, C. Xu, L. Gan, and L. Hanzo, "Low-complexity channel estimation and passive beamforming for RIS-assisted MIMO systems relying on discrete phase shifts," *IEEE Trans. Wireless Commun.*, vol. 70, no. 2, pp. 1245–1260, Feb. 2022.

[34] Q. Wu and R. Zhang, "Intelligent reflecting surface enhanced wireless network via joint active and passive beamforming," *IEEE Trans. Wireless Commun.*, vol. 18, no. 11, pp. 5394–5409, Nov. 2019.

[35] H. Alwazani, A. Kammoun, A. Chaaban, M. Debbah, M.-S. Alouini *et al.*, "Intelligent reflecting surface-assisted multi-user MISO communication: Channel estimation and beamforming design," *IEEE Open J. Commun. Soc.*, vol. 1, pp. 661–680, May. 2020.

[36] K. Zhi, C. Pan, H. Ren, and K. Wang, "Statistical CSI-based design for reconfigurable intelligent surface-aided massive MIMO systems with direct links," *IEEE Wireless Commun. Lett.*, vol. 10, no. 5, pp. 1128–1132, May. 2021.

[37] B. Di, H. Zhang, L. Song, Y. Li, Z. Han, and H. V. Poor, "Hybrid beamforming for reconfigurable intelligent surface based multi-user communications: Achievable rates with limited discrete phase shifts," *IEEE J. Sel. Areas Commun.*, vol. 38, no. 8, pp. 1809–1822, Jun. 2020.

[38] N. I. Miridakis, T. A. Tsiftsis, and R. Yao, "Zero forcing uplink detection through large-scale RIS: System performance and phase shift design," *IEEE Trans Commun*, Jan. 2023.

[39] W. Xu, J. An, C. Huang, L. Gan, and C. Yuen, "Deep reinforcement learning based on location-aware imitation environment for RIS-aided mmWave MIMO systems," *IEEE Wireless Commun. Lett.*, vol. 11, no. 7, pp. 1493–1497, Jul. 2022.

[40] T. Fang and Y. Mao, "A low-complexity beamforming design for beyond-diagonal RIS aided multi-user networks," *IEEE Commun. Lett.*, Nov. 2023.

[41] M. Nerini, S. Shen, and B. Clerckx, "Discrete-value group and fully connected architectures for beyond diagonal reconfigurable intelligent surfaces," *IEEE Trans. Veh. Technol.*, Jul. 2023.

[42] X. Jia, J. An, H. Liu, H. Liao, L. Gan, and C. Yuen, "Environment-aware codebook for reconfigurable intelligent surface-aided MISO communications," *IEEE Wireless Commun. Lett.*, vol. 12, no. 7, pp. 1174–1178, Jul. 2023.

[43] S. Shen, B. Clerckx, and R. Murch, "Modeling and architecture design of reconfigurable intelligent surfaces using scattering parameter network analysis," *IEEE Trans. Wireless Commun.*, vol. 21, no. 2, pp. 1229–1243, Feb. 2022.

[44] N. K. Kundu, Z. Li, J. Rao, S. Shen, M. R. McKay, and R. Murch, "Optimal grouping strategy for reconfigurable intelligent surface assisted wireless communications," *IEEE Wireless Commun. Lett.*, vol. 11, no. 5, pp. 1082–1086, Nov. 2021.

[45] C. Xu, J. An, T. Bai, S. Sugiura, R. G. Maunder, L.-L. Yang, M. Di Renzo, and L. Hanzo, "Antenna selection

for reconfigurable intelligent surfaces: A transceiver-agnostic passive beamforming configuration," *IEEE Trans. Wirel. Commun.*, vol. 22, no. 11, pp. 7756–7774, Nov. 2023.

[46] J. An, C. Xu, Q. Wu, D. W. K. Ng, M. Di Renzo, C. Yuen, and L. Hanzo, "Codebook-based solutions for reconfigurable intelligent surfaces and their open challenges," *IEEE Wirel Commun*, Nov. 2022.

[47] F. Wang, X. Wang, X. Li, X. Hou, L. Chen, S. Suyama, and T. Asai, "Ring-type codebook design for reconfigurable intelligent surface near-field beamforming," in *Proc. IEEE 33rd Annual International Symposium on Personal, Indoor and Mobile Radio Communications (PIMRC)*. IEEE, Sep. 2022, pp. 391–396.

[48] J. An, C. Yuen, L. Dai, M. D. Renzo, M. Debbah, and L. Hanzo, "Near-field communications: Research advances, potential, and challenges," *IEEE Wireless Commun.*, 2024.

[49] A. Abdallah, A. Celik, M. M. Mansour, and A. M. Eltawil, "Deep reinforcement learning based beamforming codebook design for RIS-aided mmWave systems," in *Proc. IEEE 20th Consumer Commun. Netw. Conf. (CCNC)*. IEEE, Mar. 2023, pp. 1020–1026.

[50] G. Wang, W. Peng, D. Li, T. Jiang, and F. Adachi, "Statistical CSI acquisition in the nonstationary massive MIMO environment," *IEEE Trans. Veh. Technol.*, vol. 67, no. 8, pp. 7181–7190, Aug. 2018.

[51] H. Yin, D. Gesbert, M. Filippou, and Y. Liu, "A coordinated approach to channel estimation in large-scale multiple-antenna systems," *IEEE J. Sel. Areas Commun.*, vol. 31, no. 2, pp. 264–273, Jan. 2013.

[52] J. An, C. Xu, D. W. K. Ng, C. Yuen, and L. Hanzo, "Adjustable-delay RIS is capable of improving OFDM systems," *IEEE Trans. Veh. Technol.*, pp. 1–16, 2024, Early Access.

[53] W. Xu *et al.*, "Algorithm-unrolling-based distributed optimization for RIS-assisted cell-free networks," *IEEE Int. Things J.*, vol. 11, no. 1, pp. 944–957, Jan. 2024.